67, 563 (1948).
9. Peaceman, D. W., Sc.D. thesis, Massachusetts Inst. Technol., Cambridge (1951).
10. Gilliland, E. R., B. F. Baddour, and P. L. T. Brian, *A.I.Ch.E. J.*, **4**, No. 2, 223 (1948).
11. Brian, P. L. T., J. F. Hurley, and E. H. Hasseltine, *ibid.*, **17**, No. 2, 226 (1961).
12. Danckwerts, P. V., *Trans. Faraday Soc.*, **46**, 300 (1950).
13. Nijsing, R. A. T. C., R. H. Hendrikse, and H. Kramers, *Chem. Eng. Sci.*, **10**, 88 (1959).
14. Perry, R. H., and R. L. Pigford, *Ind. Eng. Chem.*, **45**, 1247 (1953).
15. Brian, P. L. T., Sc.D. thesis, Massachusetts Inst. Technol., Cambridge (1956).
16. Adams, M. J., Ph.D. thesis, Univ. London (1963).
17. Thomas, W. J., and M. J. Adams, *Trans. Faraday Soc.*, **61**, No. 4, 668 (1965).
18. Thomas, W. J., and I. A. Furzer, *Chem. Eng. Sci.*, **17**, 115 (1962).
19. Thomas, W. J., and E. McK. Nicholl, *Am. J. Appl. Optics* (1965).
20. Danckwerts, P. V., and A. M. Kennedy, *Chem. Eng. Sci.*, **8**, 201 (1958).
21. Van de Vusse, J. G., *ibid.*, **16**, 21 (1961).

Manuscript received June 9, 1965; revision received March 3, 1966; paper accepted April 5, 1966.

The Dynamic Behavior of a Fixed-Bed Catalytic Reactor

FREDERIC LEDER and JOHN B. BUTT

Yale University, New Haven, Connecticut

The dynamic behavior of a fixed-bed catalytic reactor was studied under isothermal conditions by means of frequency response analysis. The investigation was conducted over a range of nonreacting and reacting conditions by using the hydrogen-oxygen combination over supported platinum as the reaction system. The kinetics of the surface catalysis of this reaction were investigated separately and then were incorporated into the analysis of frequency response data under reaction conditions.

A method was developed whereby nonlinear chemical reaction effects appearing in the frequency response measurements could be separated from hydrodynamic factors for a plug flow reactor. Use is made of the describing function technique, often used to approximate nonlinear servomechanism response, to accomplish this. It is shown by this method that Peclet numbers measured for the reacting system agree with those measured in the absence of reaction.

Based on the semitheoretical value of 2 for the Peclet group at high Reynolds numbers, a value of 0.73 sq. cm./min. was determined for the effective diffusion coefficient of hydrogen at 100°C. within the porous catalyst particles. Analysis of frequency response data in which this diffusion is not accounted for leads to Peclet numbers which are unreasonable in view of previously reported results.

Although there is a great deal of work in the recent literature on the characterization of flow and dispersion of fluids in beds of nonporous packing, and some work on porous packing, there are few data available concerning these effects under reaction conditions. Furthermore, there have been until recently no reported measurements of the dynamic behavior of a catalyst surface. It is, therefore, the primary purpose of this work to apply existing techniques of transient analysis to a study of the dynamic behavior of a fixed bed of porous catalytic particles under conditions of chemical reaction, and to define the pertinent adsorption, flow, and diffusion parameters.

Tinkler (*1*) and Sinai (*2*) have investigated by frequency response analysis related problems of flow through beds packed with inert solid in which a homogeneous chemical reaction took place in a liquid phase. Axial dispersion effects were neglected and nonlinearities were handled by Taylor series expansion. These workers studied both the temperature and concentration response in their systems; work in the present study is limited to the isothermal case.

The general problem of flow patterns and residence time in fixed beds has been considered by many workers and two distinct approaches have evolved. One considers the bed as a series of mixing cells in which the fluid in each cell is perfectly mixed and then passed on to the next cell; this approach has its most complete expression in the computational model of Deans and Lapidus (*3*). The other approach involves expression of the conservation equations as material balances over a segment of the bed in which a continuous (fluid) phase and a discontinuous (solid) phase are visualized. Numerous workers have employed this type of description; the well-known, one-dimensional, axial dispersion model of fixed beds has been thoroughly explored in the literature (*4* to *8*).

For such axial mixing or dispersion, the fundamental step in the mixing process is considered to be a random

Frederic Leder is with Esso Research and Engineering Company, Linden, New Jersey.

mixing in the interstices between particles. Experimental data on axial mixing are conveniently reported in terms of the axial Peclet number ($\bar{v}D_p/E$); Peclet numbers of 2 have been shown to correspond to mixing cells of one particle length or perfect mixing between particles. Not all experimenters, however, report $N_{Pe} = 2$ under those conditions of flow (particle Reynolds numbers > 10) where one might expect approach to perfect mixing. Carberry and Bretton (6), working with a liquid system, report Peclet numbers around 0.5 and Kramers and Alberda (8) report $N_{Pe} = 1$, also for a liquid system. The discrepancy of these results from theory has been suggested to be due to capacitance effects within the bed which cannot be adequately measured.

TRANSFER FUNCTIONS FOR BEDS OF POROUS SOLIDS IN THE ABSENCE OF REACTION

The application of frequency response analysis to flow in packed beds was introduced by Kramers and Alberda (8), who presented equations for the response of a series of perfect mixers and for a one-dimensional dispersion-plug flow model. In both cases the analysis was made for no reaction and for nonporous packing, although the treatment may be extended to beds of porous solids in which linear adsorption equilibrium exists. Experimentation on a system of the latter type under nonreacting conditions was reported by Deisler and Wilhelm (5). Use of the linear adsorption equilibrium between gas and solid implies that the appropriate mathematical description of such an experimental system must allow for the accumulation of material within the solid phase;

$$\frac{\partial q}{\partial t} = K_B \frac{\partial C}{\partial t} \tag{1}$$

For most general application, over very wide ranges of frequency, it may not be appropriate to assume gas-solid equilibrium. In the case of rapidly changing perturbations, for example, it may be necessary to relate gas phase concentration to intraparticle concentrations by means of a diffusion equation describing the rate of mass transport into and out of the solid. For a simplified geometry

$$D_s \nabla^2 q = D_s \frac{\partial^2 q}{\partial x^2} = \frac{\partial q}{\partial t} \tag{2}$$

where x may be taken as the volume-to-surface ratio of the particle. We incorporate this equation into the series of mixers model to obtain an overall description of the fixed bed of porous particles. For cell i of the series

$$V(C_{i-1} - C_i) = V_1 \frac{\partial C_i}{\partial t} + V_2 \frac{\partial q_i}{\partial t} \tag{3}$$

where

$$V_1 = \frac{A_x \epsilon L}{N} \tag{4}$$

$$V_2 = \frac{A_x L\,(1-\epsilon)}{N}$$

By material balance

$$V_2 \frac{\partial q}{\partial t} = \int_S D_s \left(\frac{\partial q}{\partial x}\right)_S dS = D_s A_D \left(\frac{\partial q}{\partial x}\right)_S \tag{5}$$

Accumulation within the solid may be defined by the surface integral of the transport at the surface. Transforming Equation (2) with respect to time, one obtains

$$D_s \frac{d^2 \hat{q}}{dx^2} = s\hat{q} \tag{6}$$

where

$$q(x, o) = 0$$

Solving

$$q = A_1 \exp\left[-\sqrt{\frac{s}{D_s}}\, x\right] + A_2 \exp\left[\sqrt{\frac{s}{D_s}}\, x\right] \tag{7}$$

The boundary conditions are

$$\hat{q} = \hat{C} \text{ at } x = x_p \tag{8}$$
$$d\hat{q}/dx = 0 \text{ at } x = x_p/2$$

Evaluation of constants A_1 and A_2 and rearrangement yield for the concentration gradient

$$\left(\frac{d\hat{q}}{dx}\right)_{x=x_p} = \hat{C}\sqrt{\frac{s}{D_s}}\left(\tanh\sqrt{\frac{s}{D_s}}\, x_p\right) \tag{9}$$

Therefore, by substitution into the transform of Equation (5)

$$V_2 s\hat{q} = D_s A_D \hat{C}\sqrt{\frac{s}{D_s}}\left(\tanh\sqrt{\frac{s}{D_s}}\, x_p\right) \tag{10}$$

The transfer function for one cell is, from Equations (3) and (10)

$$G_i(s) = \frac{\hat{C}_i}{\hat{C}_{i-1}} = \left[1 + \frac{A_x \epsilon L}{NV} s + \frac{D_s A_D}{V}\sqrt{\frac{s}{D_s}}\left(\tanh\sqrt{\frac{s}{D_s}}\, x_p\right)\right]^{-1} \tag{11}$$

For the bed composed of N such cells

$$G_T(s) = \left[1 + \frac{A_x \epsilon L}{NV} \cdot s + \frac{D_s A_D}{V}\sqrt{\frac{s}{D_s}}\left(\tanh\sqrt{\frac{s}{D_s}}\, x_p\right)\right]^{-N} \tag{12}$$

By way of comparison, for a nonreacting system in which adsorption equilibrium between fluid and solid may be assumed [Equation (1)], the transfer function is

$$G_T(s) = \left[1 + \frac{A_x \epsilon s L}{NV}\left(1 + K_B \cdot \frac{1-\epsilon}{\epsilon}\right)\right]^{-N} \tag{13}$$

THE DESCRIBING FUNCTION ANALYSIS FOR NONLINEAR KINETICS

The approaches detailed above do not specify a reaction rate form; the inclusion of linear rate terms is easily accomplished, but if the rate is proportional to higher powers of the concentration, transform techniques are no longer applicable and an alternative route to frequency response analysis must be sought. In this work the describing function method was found useful in obtaining an appropriate description of frequency response under the influence of such nonlinear chemical reaction phenomena.

The describing function, defined by analogy to the transfer function, is based on the principle of Fourier series representation where the assumption is made that only the first harmonic in the output is significant (9). In physical application this is often a good assumption if the nonlinear device is in series with linear devices which damp the higher harmonics. In the present use, only the reaction rate term is nonlinear; the reactor itself is inherently a linear device.

For a second-order chemical reaction taking place in a plug flow reactor, the appropriate differential equation is

$$-\bar{v}\frac{\partial C}{\partial l} - k_r C^2 = \frac{\partial C}{\partial t} \tag{14}$$

Since for the plug flow reactor each element of fluid has the same residence time as any other element of fluid, the phase lag between output and input is simply the residence time in the reactor multiplied by the frequency of the forcing function. Also, for the plug flow reactor, an input forcing function is not attenuated by the flow through the reactor if boundary-layer or pore diffusion effects are negligible; the only forcing signal attenuation which occurs is caused by chemical reaction during residence within the reactor. For a second-order reaction, the conversion under steady state conditions is

$$\frac{C_{OUT}}{C_{IN}} = \frac{1}{1 + k_r \theta C_{IN}} \tag{15}$$

According to the analysis of forcing signal attenuation, the effluent concentration [actually a solution to Equation (14)] from a plug flow reactor must be

$$C(t) = \frac{C_{IN}(t-\theta)}{1 + k_r \theta C_{IN}(t-\theta)} \tag{16}$$

The input and output concentration functions may be written as the sum of a sinusoid and a mean concentration level:

$$C(t)_{IN} = A_o + B_o \cdot \sin \omega t \tag{17}$$

$$C(t)_{OUT} = A + B \cdot \sin \omega t \tag{18}$$

It is more convenient in frequency response analysis to eliminate the mean concentration level contribution to input and output functions; thus a new effluent function will be defined which is equal to the actual effluent function minus the mean concentration level [A_o or A in Equations (17) and (18)]. The mean output level is equal to the mean input level attenuated by reaction according to Equation (15). The new function is then given by

$$F(t) = \frac{A_o + B_o \sin \omega(t)}{1 + k_r \theta[A_o + B_o \sin \omega(t)]} - \frac{A_o}{1 + k_r \theta A_o} \tag{19}$$*

which represents the total reactor effluent minus the mean effluent level. The system response given in Equation (19) may be represented by a Fourier series and the first harmonic compared to the input function to determine frequency response characteristics, which is the essence of describing function analysis. For response to concentration forcing about a mean level

$$C(t)_{IN} = B_o \sin \omega t \tag{20}$$

$$C(t)_{OUT} = F(t) \tag{21}$$

and

$$F(t) = \sum_{n=o}^{\infty} B_n \sin \omega t \tag{22}$$

where

$$B_1 = \frac{2}{\pi} \int_o^{\pi} F(t) \sin(\omega t)\, d(\omega t) \tag{23}$$

The amplitude of the first harmonic B_1 is defined by Equation (23) and (B_1/B_o) is the amplitude ratio of the response function. Numerical values are obtained on substitution of Equation (19) into Equation (23) and evaluation of the integral. The describing function technique is simply a type of linearization, and for specified forcing frequency and amplitude the method is identical to a linear transfer function. However, variations in input amplitude can cause changes in amplitude ratio and phase lag in nonlinear systems, and this effect is specified by the describing function.

* t is the independent variable instead of $(t - \theta)$. The only error introduced by this simplification is in phase lag; however this calculation is carried out only for amplitude attenuation and is independent of the shift in time axis.

EXPERIMENT

The hydrogen-oxygen reaction over supported platinum catalyst was employed as the reacting system for this study. In design of a transient response study the speed of chemical analysis dictates both the type of transient and the reactor size. For the present study a suitable continuous chemical analysis was not available, so pulse or step function perturbations were abandoned in favor of frequency response. The reactor was sized so that the shortest period sine waves employed in experimentation would, in fact, be of the order of average residence time in the reactor and a dilute catalyst was fabricated, based on reactor size and available kinetic data.

The reactor system consisted ultimately of 130 ft. of 7/16-in. I.D. aluminum tubing packed with 3,100 g. of porous eta alumina extrudates on which 14.5 mg. of platinum were supported. Tube-to-particle diameter ratio within the bed was approximately 6:1. Further details of catalyst fabrication and properties are given elsewhere (*10*). The catalyst was sufficiently dilute to eliminate problems of temperature gradients both within pellets and within the reactor. Experimentation was conducted at a bed temperature of 100°C.; temperature control was provided by steam jacketing around the reactor and isothermal operation was verified by measurements of temperature along the length of the reactor which indicated less than 0.1°C. variation from the jacket temperature for any of the runs made. Since the inlet gas to the reactor was never more than 3% hydrogen, volume changes on reaction were negligible.

In Figure 1 a diagram of the reactor system is given. Compressed air was regulated to 64 lb./sq.in.abs., mixed with the modulated hydrogen steam, and fed through the catalyst bed. The flow was measured by an outlet bubble meter. Inlet and outlet pressure and concentration were measured, as well as the bed temperature at several places in the bed. Concentration measurements were made by gas chromatographic analysis of continuous sample streams. Details of the equipment and the sampling procedure are given elsewhere (*11*).

The sine waves were generated by passing the hydrogen stream through a very fine metering valve, modified with close tolerance bearings. The stem of the valve had a spur gear which was attached to an eccentric cam which was actuated by a variable speed motor. The volume change of the total feed gas stream was negligible, since the hydrogen stream comprised only a small fraction of the total flow.

The two sample streams were passed through a four-way valve where one stream was selected for analysis and the other was vented. The sample stream was then fed into a Beckman gas sample valve which was actuated automatically by a solenoid valve and a pneumatic piston.

Measurement of the amplitude attenuation and phase lag of the effluent concentration was carried out over the range of frequencies from 1 cycle/30 min. to 2 cycles/min. This policy established a range of frequencies whose wavelengths varied approximately from one half to thirty times the average reactor residence time.

Frequency studies were carried out over a range of particle Reynolds numbers from 6 to 86 in order to determine the

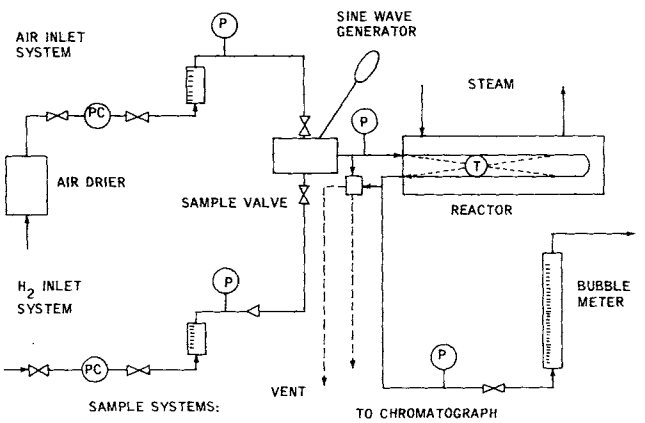

Fig. 1. Schematic of reactor system.

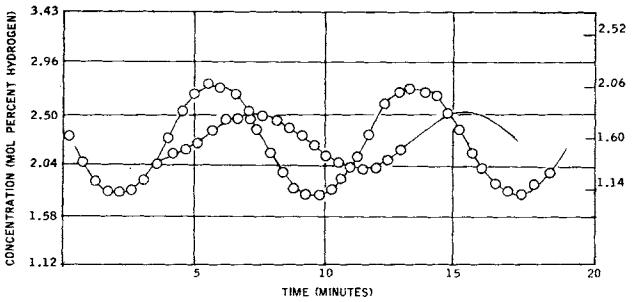

Fig. 2. Example of forcing and effluent sinusoids; run TR-5.

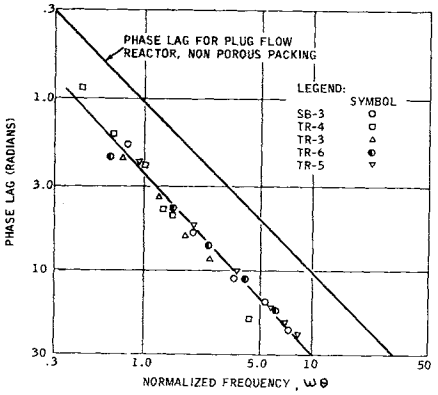

Fig. 3. Phase lag.

effect of variation in flow conditions on the reactor response. Additional measurements were made on a short bed (42 ft.) in order to confirm measurements of capacitance effects in the longer bed. Data were also obtained under nonreacting conditions and at lower amplitudes in order to obtain independent information on the mixing characteristics. Normally the amplitude of an input sine wave was 18% of the mean concentration level, from midpoint to peak. Lower amplitude runs were made at 12% of the mean level, or 66% of normal amplitude. Figure 2 presents an example of the wave forms under consideration; the data points are spaced 30 sec. apart in this run. Fourier analysis of the experimental forcing functions was carried out for a number of runs (*11*); the total distortion of the input waves varied between 5.7 and 8.1%, while output waves had an average of only 2% total distortion, indicative of some filtering effect in the packed bed.

Measurement of high frequency sinusoids posed a particular problem, the solution of which is noteworthy. The chromatographic analysis and sampling technique were constrained to take no more than one sample every 30 sec. It was desired to measure frequencies as high as 1 cycle/30 sec., so the frequency of the sinusoid was adjusted to 1 cycle/33 sec. This permitted samples to be taken at a constant interval approximately equal to 90% of one period. The result of this procedure is the production of a secondary wave with a period ten times the parent wave. The secondary wave can be clearly defined with ten data points. A similar procedure was used to develop a secondary wave corresponding to a frequency of 1 cycle/min

The ranges of variables and experimental conditions investigated in this study are summarized in Table 1.

FREQUENCY RESPONSE RESULTS AND ANALYSIS

In Figure 3 are presented measured phase lags for experimentation at various Reynolds numbers and both bed lengths investigated. These data are representative of all the phase lag results and are presented as a function of the frequency of the forcing function normalized with respect to contact time in the bed. Over the full range of Reynolds numbers investigated, from 6.7 to 86, no difference is noted in the phase lag at any given frequency. The phase lag is seen to be 2.6 times the normalized frequency, constant over the range of investigation. This phase lag, according to the plug flow reactor model, is the result only of capacitance in the porous solid packing, as expressed in Equation (13). [Reaction affects amplitude attenuation but not phase lag, as indicated in Equation (16).] The lag corresponds precisely to the factor $\left(1+\frac{1-\epsilon}{\epsilon}K_B\right)$ in this equation. The porosity ϵ was determined for the experimental reactor as 0.31 in separate experimentation (*11*), and K_B was computed from the phase lag results as 0.74.

Table 1. Summary of Frequency Response Experiments

Run No.	$\omega\theta$	N_{Re}**	θ, min.
TR-1*	1.6-11.1	34.0	2.58
TR-2	1.3-79.3	32.7	2.70
TR-3	0.6-50.3	48.0	1.55
TR-4	0.4-25.4	86.3	0.82
TR-5	2.4-70.0	19.8	4.55
TR-6†	1.7-10.0	27.7	3.25
TR-7	0.8-7.7	48.0	1.71
SB-1*, †	0.3-18.1	50.0	0.58
SB-2	0.3-19.4	46.5	0.63
SB-3	5.3-18.9	6.75	4.46
SB-4‡	0.2-2.9	48.0	0.59

* TR series in 130-ft. reactor, SB series in 42-ft. reactor. All runs at 100°C.
† No reaction on this run.
‡ Input amplitude 12% of mean. All other runs at 18%.
** Based on particle dimensions.

The analysis of amplitude attenuation results is not so straightforward, since the effects of chemical reaction are of primary importance here. In work reported elsewhere (*10*) the kinetics of the chemical reaction between hydrogen and oxygen are defined for the conditions of this study. A rate equation based on the mechanism of reaction between chemisorbed oxygen and gas phase hydrogen describes the conversion data obtained in the experimentation on kinetics. The rate equation proposed is

$$R_{H_2} = -\frac{1}{\rho\pi}\frac{K_r K_o P_H^2 P_o}{(1 + K_o P_o + K_w P_w)} \qquad (24)$$

Under the conditions of experimentation employed in the frequency response study, $P_o >> P_H$ and $P_o >> P_w$. The rate equation simplifies under these conditions to an approximate second-order form:

$$R_{H_2} = k_r' C_H^2 \qquad (25)$$

In order to interpret amplitude attenuation data with respect to the reaction, two types of information are required. First, one must determine the steady state conversion level, that is, k_r' in Equation (25). Second, the relationship between the steady conversion level and transient amplitude attenuation must be determined. The steady state conversion is defined for the second-order reaction by Equation (15), and the transient output for that value of k_r' and θ by the describing function analysis by employing Equation (19). The ratio of the amplitude attenuation so determined to steady state conversion is defined as the *describing factor* and is immediately determinable for a given system on specification of the forcing amplitude.

The procedure employed in this investigation was to normalize the observed amplitude attenuations with respect to the describing functions computed for conditions of the individual experimental runs. Hence

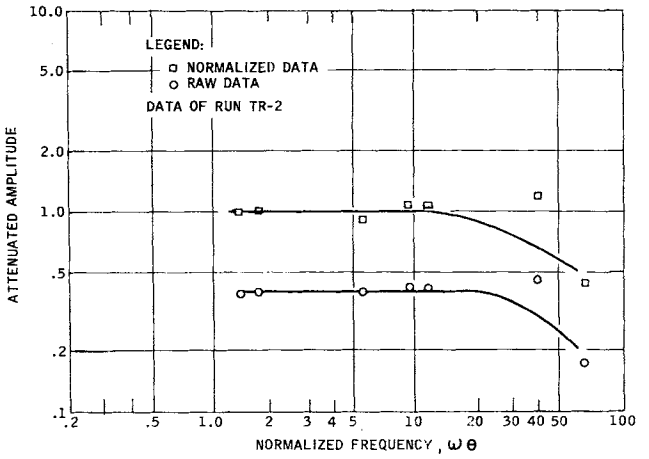

Fig. 4. Amplitude attenuation and the effect of normalizing with respect to the describing factor and the mean conversion.

$$(B/B_o)_N = (B/B_o)/(B_1/B_o) \qquad (26)$$

where B_1/B_o is the calculated describing function. It is a notable result, as shall be seen in the subsequent presentation of these data, that this method of normalization raises the amplitude attenuation to the nonreactant level over the entire range of Reynolds numbers, permitting direct comparison with amplitude attenuation in nonreacting systems. In essence, the effects of reaction are removed from the analysis, leaving only the hydrodynamic effects within the bed to be considered in interpretation of the normalized data.

Figure 4 shows, as an example, the amplitude attenuations measured for run TR-2, and the same data normalized as described above. In Figure 5*a* are given normalized amplitude attenuation results from four runs in which data from reacting and nonreacting systems are compared, in both the long bed and the short bed employed in experimentation. No differences are noted between the normalized reaction data and data of nonreacting runs. After such normalization, then, the results should be amenable to analysis with some appropriate mixing model *without* chemical reaction. This indeed is true; the solid line of Figure 5*a* is computed from Equation (13) for a reactor model (long bed) of 1,000 mixing cell units; the results are identical to those computed from Equation (12) for $N = L/D_p$ and $D_s = 0.73$ sq. cm./min. A discussion of the significance of the interpretation employing these two models is given subsequently. The decrease in attenuated amplitude for $\omega\theta > 10$, which is observed experimentally, is predicted by the computation, indicating that deviations from ideal flow behavior may be important in this region.

In Figure 5*b* are compared amplitude attenuation data at the same Reynolds number for the two bed lengths investigated. No difference in these data is noted which can be attributed to an effect of bed length, although in the region of $\omega\theta > 10$ there are few short bed data. The curve in this figure is again that computed from Equation (12) or (13).

A comparison of amplitude attenuation in the two bed lengths at the same contact time is given in Figure 6*a*. The scatter in these data results primarily from the experimental error involved in carrying out transient experiments at very low flow rates (the two runs involved hydrogen flow rates of approximately 10 and 30 cc./min. through the experimental equipment); within the precision of experimentation (*11*) there is no effect on conversion due to change in bed length.

Figures 6*b* and 7 present the results of experimentation on the effect of flow rate on the reactor response. Runs TR-4, TR-5, and SB-3, given in Figure 6*b*, represent data obtained at the extremes of Reynolds numbers investigated, namely, 6.7 and 86; there is no effect on amplitude attenuation. In Figure 7 are plotted amplitude attenuations at normalized frequencies of 20 and 40 for a number of runs. The functional dependence on Reynolds number is seen to be negligible. This implies similar mixing characteristics in the bed at the extremes of flow conditions examined, and indicates the absence of boundary layer diffusional limitation in the reacting system.

DISCUSSION

The describing function technique was found to be a useful means of normalizing frequency response data

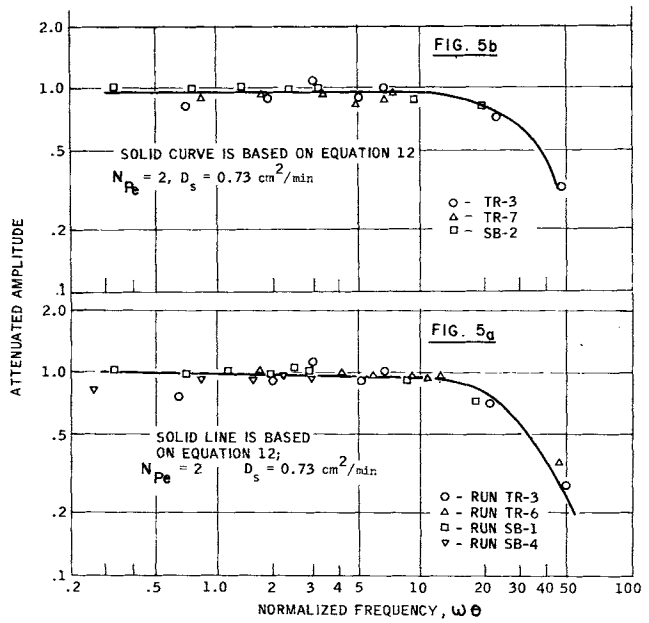

Fig. 5. (*a*) Comparison of reacting and nonreacting flow patterns at several bed lengths, amplitudes, and Reynolds numbers. (*b*) Comparison of amplitude attenuation at several bed lengths and the same Reynolds number.

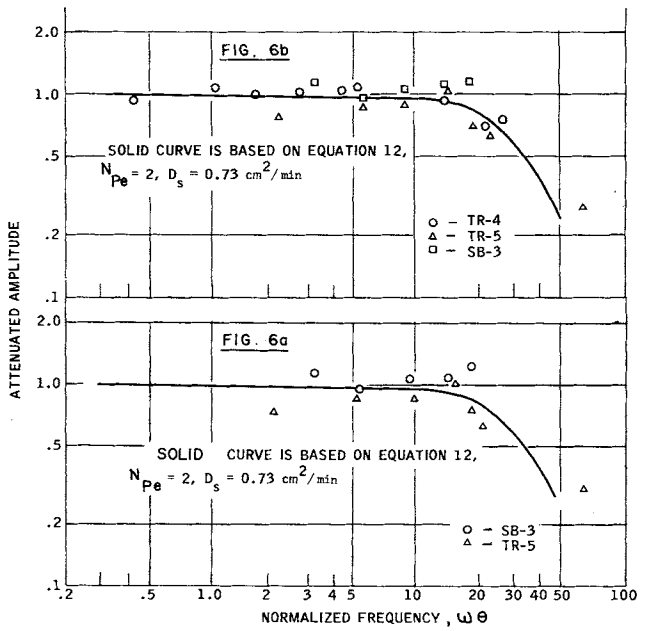

Fig. 6. (*a*) Amplitude attenuation at the same contact time in beds of different length. (*b*) Amplitude attenuation at extremes of Reynolds numbers and two bed lengths.

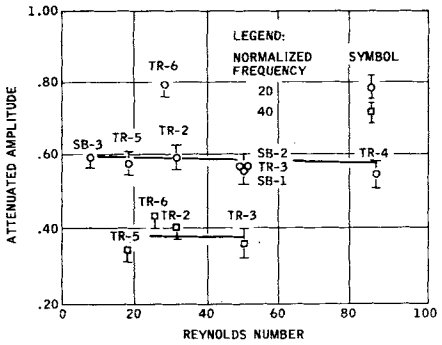

Fig. 7. Attenuated amplitudes at selected frequencies.

under these isothermal conditions for direct comparison with nonreacting data. Since no attempt is made to incorporate any sort of mixing into the describing function analysis, it is quite noteworthy that the method can reconcile data for reacting and nonreacting systems over a very wide range of experimental variables where dispersion in the fluid phase and capacitance in the solid phase may have significant effect on the attenuation. This method appears to provide a means of handling at least simpler forms of nonlinear kinetics in frequency response experimentation; in such cases reaction effects are separable from the mixing characteristics of the bed and nonreacting theories of fixed bed behavior may be applied to the reacting system.

The describing function employed here, based on a piston flow assumption, calculates amplitude attenuation due to reaction independent of the mixing characteristics of the system. Data are measured on the combined effects of mixing and reaction, as well as on the mixing effects alone; therefore by appropriately removing the effects of chemical reaction in a reacting system, one can compare the mixing characteristics of reacting and nonreacting systems. These effects were found to be identical under isothermal circumstances; no additional amplitude attenuation was found to occur as a result of chemical reaction in a dispersive system.

The phase lag measurements reported in Figure 3 are linear with the normalized frequency over the range investigated. The proportionality constant β relating the phase shift to the normalized frequency is an important factor in predicting breakthrough of a step function from the bed. The linear phase shift can be interpreted to mean that a step or pulse will elute from the bed with its peak eluting at time $\beta\ L/\bar{v}$ after input, and results from the presence of porous packing which is not inert with respect to the fluids passing through the bed.

The phase lag data are, however, not very informative with respect to the flow patterns within the bed. In developing Equation (13), we have employed a model which may denote various degrees of mixing in the bed, depending on the number of mixing cells included in the reactor, for computing the curves given in Figures 5 and 6. The correlation of this series of mixers model (7) in terms of axial dispersion coefficients is

$$\frac{L}{D_p} \cdot \left(\frac{1}{N}\right) = \frac{2}{N_{Pe}} \tag{27}$$

Based on the experimental particle sizes and the value of N (1,000) which best reproduced the experimental amplitude attenuation characteristics, a Peclet number of approximately 0.13 is calculated. Though there are little data on axial mixing in beds of porous packing, this result seems to disagree markedly with prior studies employing gaseous fluids. It is evident that at the high frequencies, where amplitude attenuations are large, the rate of transport within the porous particles is not sufficient to allow attainment of gas-solid equilibrium and the single axial dispersion coefficient cannot be used to characterize the system completely. One must, in addition, account for the diffusion of material in and out of the solid phase.

This effect is described more completely as follows. Under steady state conditions it can be shown (*12*) that no appreciable diffusional gradients exist within the catalyst particles as a result of chemical reaction. Under low-frequency oscillation, these diffusional gradients must also be negligible; however, at some sufficiently high frequency the diffusional concentration gradients must become appreciable, due to the inability of the internal concentration to respond instantaneously to the external changes. At this point the fluid phase concentration can no longer be linearly related to the solid phase concentration. For the interpretation of experimental frequency response data using the series of mixers pore diffusion model [Equation (12)] which represents this case, it is reasonable to establish the fluid phase mixing at a level consistent with prior observation for the experimental conditions employed and to obtain pore diffusion effects by means of fitting computed results to experimental data.

The effective area available for diffusional transport in this model is the area of each particle multiplied by the number of particles in each mixing cell and a geometric factor which is a function of particle shape and distribution within the bed. The shape factor [incorporated in A_0 in Equation (12)] is evaluated iteratively; in order to satisfy both phase lag and amplitude attenuation data it was found that approximately 50% of the total pellet external area was effective in transport. The computed curve for a Peclet number of 2 and an effective diffusivity of hydrogen within the solid of 0.73 sq. cm./min. is shown in Figure 8. This curve is identical to those computed from Equation (13), as mentioned previously, for the unrealistic value of $N_{Pe} = 0.13$. The calculated diffusivity of 0.73 sq. cm./min. is in general accord with previously reported values for diffusivities within porous structures.

In Figure 8 are also given computed amplitude attenuations for the system with a diffusivity of 0.73 sq. cm./min. for various values of the Peclet group. The distinction between N_{Pe} of 2 and N_{Pe} of 0.5, essentially the limits of data reported on Peclet numbers under conditions of well developed turbulence, is small. It may thus be concluded that amplitude attenuation is not very sensitive to N_{Pe} in this range and that such measurements may provide a

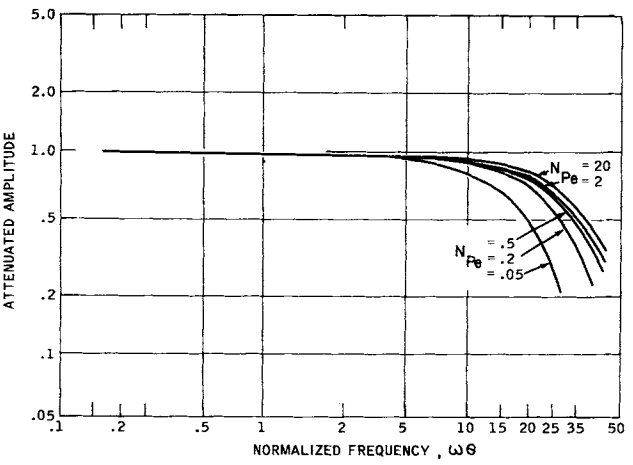

Fig. 8. Calculated amplitude attenuation at several values of Peclet number for a porous solid diffusivity of 0.73 sq. cm./min.

reasonable means for determination of effective diffusivities within porous solids.

CONCLUSIONS

The describing function technique is shown applicable for characterization of the dynamic behavior of a chemical reactor in response to concentration forcing where a nonlinear kinetic law prevails. If the steady state conversion in the reactor is known, providing sufficient information to evaluate the parameters of the rate law, the transient output can be expressed in a Fourier series, the first term of which is employed in representation of the frequency response of the nonlinear system. The near plug flow conditions prevailing in the reactor during experimentation allow separation of the chemical kinetics from the mixing effects in analysis of measured amplitude attenuation data, indicating that attenuation of the system is a linear combination of the two effects under such conditions.

Interpretation of the response data in terms of a mixing cell porous capacitance model yields reasonable values for effective diffusivities within the solid based on the assumption of $N_{Pe} = 2$ to describe dispersion effects at the high Reynolds numbers employed in experimentation. At high forcing frequencies diffusion into the capacitance within the porous support structure of the catalyst is quite important in determining amplitude attenuation characteristics.

A simplified model employing a series of mixing cells and the assumption of linear equilibrium $q = K_B C$ can provide adequate representation of experimental amplitude attenuation and phase lag data (β measured from the latter is equal to: $\beta = K_B(1-\epsilon)/\epsilon$ at lower forcing frequencies and with reasonable values of Peclet number.* In order to fit experimental amplitude data at normalized frequencies of the order of 10 rad. or greater, however, the simple model requires unrealistic values of the Peclet number and provides only an empirical correlation of experimental results. This underscores the point that the axial dispersion interpretation is capable of explaining effects based on the mixing of fluid within the interstices of the packing, but care must be exercised in attempting to apply this model to effects caused by other phenomena such as radial gradients of concentration or velocity or diffusion in or out of porous or stagnant areas.

ACKNOWLEDGMENT

The authors express their appreciation to the American Machine and Foundry Corporation, the Du Pont Corporation, the Continental Oil Corporation, and Yale University for their financial support of this project. The authors are also grateful to Professors Reuel Shinnar and J. J. Carberry for their helpful opinions concerning the treatment and presentation of the data.

NOTATION

A_X = cross-sectional area of the reactor
A_o = mean level of input sinusoid
A = mean level of output sinusoid
A_1, A_2 = constants of Equation (7)
A_D = area available for diffusion into a pellet
B = amplitude of output function
B_o = amplitude of sinusoidal forcing function
B_1 = amplitude of the first harmonic defined by Equation (23)
C = concentration in gas phase
$\hat{C}$ = transform of gas concentration
D_s = effective diffusivity within porous solid
D_p = particle diameter
E = axial dispersion coefficient
$F(t)$ = output function
G = mass flow rate based on total cross section
$G(s)$ = transfer function
i = mixing cell
K_o = adsorption equilibrium constant for oxygen
K_w = adsorption equilibrium constant for water vapor
K_B = constant relating the gas and solid phase concentrations
k_r', k_r = reaction rate constant
K_r = reaction rate constant for hydrogen-oxygen reaction
L = length of the reactor
l = length variable
N = number of mixing cells
N_{Pe} = Peclet group ($\bar{v}D_p/E$)
P_H = partial pressure of hydrogen
P_o = partial pressure of oxygen
q = concentration within solid
$\hat{q}$ = transform of concentration within solid
N_{Re} = Reynolds number based on particle dimensions, $N_{Re} = (D_p G/\mu)$
R_{H_2} = rate of hydrogen conversion
S = particle external surface
s = Laplace transform variable
t = time
$\bar{v}$ = linear gas velocity
V = volumetric velocity
X = volume to surface ratio variable for individual particle
x_p = particle length, volume to surface ratio

Greek Letters

β = $(1 + [(1-\epsilon)/\epsilon]\, K_B)$
ϵ = bulk porosity of bed
θ = residence time
π = total pressure
μ = viscosity
ω = frequency
ρ = molal density

LITERATURE CITED

1. Tinkler, J. D., Ph.D. dissertation, Univ. Delaware, Newark (1963).
2. Sinai, Jose, Ph.D. dissertation, Univ. California, Berkeley (1965).
3. Deans, H. A., and Leon Lapidus, *A.I.Ch.E. J.*, **6**, 656 (1960).
4. McHenry, R. H., and R. H. Wilhelm, *ibid.*, **3**, 83 (1957).
5. Deisler, P. F., and R. H. Wilhelm, *Ind. Eng. Chem.*, **45**, 1219 (1953).
6. Carberry, J. J., and R. H. Bretton, *A.I.Ch.E. J.*, **4**, 367 (1958).
7. Sinclair, R. J., and C. E. Potter, *Trans. Inst. Chem. Engrs. (London)*, **43**, T3 (1965).
8. Kramers, H., and G. Alberda, *Chem. Eng. Sci.*, **2**, 173 (1953).
9. Thaler, G. J., and R. G. Brown, "Analysis and Design of Feedback Control Systems," 2 ed., McGraw-Hill, New York (1960).
10. Leder, Frederic, and J. B. Butt, *A.I.Ch.E. J.*, **12**, No. 4, 718 (1966).
11. Leder, Frederic, Ph.D. dissertation, Yale Univ., New Haven, Conn. (1965).
12. Weisz, P. B., *Z. Phys. Chem.*, **11**, 1 (1957).

Manuscript received October 24, 1965; revision received April 19, 1966; paper accepted April 20, 1966. Paper presented at A.I.Ch.E. Philadelphia meeting.

* It should be apparent from experimental results that there is little difference between plug flow or either the mixing cell porous capacitance or mixing cell linear equilibrium models with $N_{Pe} = 2$ for all Reynolds numbers in the range of normalized frequency $\omega\theta < 10$. These models are essentially the same in this region.